Supplemental Material

NilD CRISPR RNA contributes to *Xenorhabdus nematophila* colonization of symbiotic host nematodes

Jeff L. Veesenmeyer, Aaron W. Andersen, Xiaojun Lu, Elizabeth A. Hussa, Kristen E. Murfin, John M. Chaston, Adler R. Dillman, Karen M. Wassarman, Paul W. Sternberg, and Heidi Goodrich-Blair

Supplemental Table 1. Regions of genome differences between XnSc 081 and XnSc 800

Mutation	Gene ID	Gene name/Function	Effect on Coding Sequence
SNVS			
T241,233C	XNC1_0274	*fabR*, transcriptional repressor fragment	Synonymous
G241,237C	XNC1_0274		Synonymous
T270,582G	XNC1_0323	*rpsC*, 30S ribosomal subunit protein S3	H139Q
A270,617T	XNC1_0323		E151V
C270,642T	XNC1_0323		Synonymous
C270,880G	XNC1_0324	Hypothetical	Synonymous
C270,896A	XNC1_0324		Q40K
T270,940G	XNC1_0325	*rlpP*, 50S ribosomal subunit protein L16	V8G
T636,807G	XNC1_0743	*oppA3*, ABC Transporter family	D2E
A653,167T	Upstream of XNC1_0754	ahpC, alkyl hydroperoxide reductase	NA[1]
T804,168G	XNC1_0935	Hypothetical	M15L
C941,069A	XNC1_1064	*lpxC*, NAG deacetylase	NA
T941,071A	XNC1_1064		
T941,131G	XNC1_1064		V15G
T976,807A	XNC1_1092	Hypothetical	Y40*
C1,065,676A	Upstream XNC1_1197	e14 prophage tail fiber protein	NA
G1,081,851C	Downstream XNC1_1212	Phage modular protein D	NA
G1,081,856C	Downstream XNC1_1212		NA
T1,081,865C	Downstream XNC1_1212		NA
G1,081,878C	Downstream XNC1_1212		NA
T1,081,884,G	Downstream XNC1_1212		NA
T1,081,890G	Downstream XNC1_1212		NA
T1,195,432C	XNC1_1332	*mrd*, peptidoglycan synthetase	K195E
A1,422,830T	XNC1_1543	*infA*, Protein chain initiation factor	L8*
C1,422,833T	XNC1_1543		G7D
C1,712,985T	XNC1_1774	Hypothetical	With Below Q44S
A1,712,986C	XNC1_1774		Q44S
A2,598,811T	Downstream XNC1_2635	NA	NA
G2,898,177A	XNC1_2903	DnaG primase like seq	Synonymous
G2,982,740A	Upstream of XNC1_2997	Chiting binding protein	NA
T3,490,398G	XNC1_3605 Operon	GroEL chaperone operon	NA
C3,490,857G	XNC1_3606 Operon	GroEL chaperone operon	NA
T3,495,578A	Downstream XNC1_3616	BamHI control element	NA
G3,704,993A	XNC1_3848	*pcm*	Q156*
G3,839,515A	Upstream XNC1_3977	Hypothetical	NA
T3,839,518A	Upstream XNC1_3977		NA
T3,839,519A	Upstream XNC1_3977		NA
A3,839,525C	Upstream XNC1_3977		NA
A3,839,526G	Upstream XNC1_3977		NA
A3,839,634G	XNC1_3978	*gmhB*	C156R
A3,839,640G	XNC1_3978		F154L
C3,839,695T	XNC1_3978		Synoymous
G3,839,718T	XNC1_3978		L128M
T3,839,751A	XNC1_3978		M117L
C3,933,193G	XNC1_4062	*imp*, organic solvent tolerance protein	Synonymous
G3,933,205T	XNC1_4062		K246N
A3,933,207T	XNC1_4062		N247I
G3,933,223T	XNC1_4062		E252D

C3,933,272A	XNC1_4062		H269N
A4,204,557T	XNC1_4379	*rpoB*, RNA polymeras subunit	D516V
Frameshift Mutations			
-36,438A	XNC1_0034	*gidA*, glucose-inhibited division protein	G19fs
-241,252A	XNC1_0274	*fabR*, transcriptional repressor	NA
A270,818-	XNC1_0324	*rpsC*, 30S ribosomal subunit protein S3	E218fs, K14fs
C270,859-	XNC1_0324		G27fs
C270,868-	XNC1_0324		V30fs
C270,875-	XNC1_0324		Q33fs
C270,890-	XNC1_0324		P38fs
-653,167T	Upstream XNC1_0753	*ggt*, gamma glutamine transpeptidase	NA
G653,171-	Upstream XNC1_0753		NA
G655,360-	XNC1_0757/0758	S-adenosylmethionine tRNA riobsyltransferase	NA
T940,085	XNC1_1062	Tubulin-like GTP-binding protein/GTPase	NA
A976,820-	Upstream XNC1_1093	*MscS*, mechanosensitive channel protein	NA
-976,832A	Upstream XNC1_1093		NA
-1,081,791T	Downstream XNC1_1212	Phage modular protein D	NA
A,1081,795-	Downstream XNC1_1212		NA
A1,081,807-	Downstream XNC1_1212		NA
A1,130,532-	Upstream tRNA-Ser	NA	NA
-1,422,844T	XNC1_1543	infA	H4fs
T1,496,524-	Upstream XNC1_1603	Hypothetical	NA
G1,496,534-	Upstream XNC1_1603		NA
A2,027,395-	Upstream XNC1_2116	Putative potassium transport	NA
G3,490,877-	XNC1_3606 Operon	GroEL chaperone	NA
A3,490,907	XNC1_3606 Operon	GroEL chaperone	NA
T3,490,920	Promoter upstream XNC1_3607	GroEL chaperone	NA
G4,429,599	Promoter upstream XNC1_4642	*mnmE*, GTPase involved in tRNA modification	NA

[1]NA indicates a mutation that does not affect the coding sequence of any predicted open reading frame

Supplemental Table 2. CRISPR loci of *X. nematophila* (HGB800) designated alphabetically according to their chromosomal position.

CRISPR Region	Coordinates (HGB800 genome)	Repeat #	Notable features
A	881776-882019	2	Spacer identical to that of CRISPR-B
B	1814239-1814329	2	Spacer identical to that of CRISPR-A. Encoded near 3' end of repeat region C.
C	1814463-1815955	25	Spacer 22 is 100% identical to XNC1_3681, a XnSc chromosomal gene of unknown function
D	3320125-3320276	3	Highly divergent repeat sequence
E	3577918-3579107	20	CAS-proximal (upstream); Spacer 4 is 100% identical to XNC1_2560 (*xptE1)*, a XnSc chromosomal gene predicted to encode an A subunit of Tc toxin
nilD	3579434..3579491	2	Necessary for nematode colonization
G	3589391_3590272	16	CAS-proximal (downstream)

Supplemental Table 3: Colonization analysis of HGB315 (*nilD6*::Tn*5)* carrying SR2 deletion constructs[a]

Plasmid	*orf1*	*orf2*	RNA	XnSc 081 wild-type	XnSc 081 *nilD6*::Tn*5*
pBCSK+	n.a.	n.a.	n.a.	37.3 ±12.3	0.8 ± 0.1
pSR2-312	+	+	+	38.3 ± 13.3	43.6 ± 16.5
pSR2-ΔR90	-	+	+	31.9 ± 2.2	49.1 ± 23.9
pSR2-ΔR126	-	+	-	53.8 ± 23.7	0.1 ± 0.0
pSR2-ΔL84	+	-	+	18.7 ± 5.4	90.3 ± 43.8
pSR2-ΔL132	+	-	+	15.6 ± 4.5	40.9 ± 23.5
pSR2-ΔL161	+	-	-	40.3 ± 20.6	0.1 ± 0.0
pSR2-ΔR90/ΔL84	-	-	+	32.1 ± 11.4	53.4 ± 4.0

a. Each construct was tested 3 independent times and colonization data represent average cfu/IJ ± standard error.

Supplemental Table 4: Oligonucleotides used in this study

Name	Sequence (5'-3')
PCR Amplification and Sequencing	
KHP36N	CATGGCTACTTTGAATTTCC
KHP55	ATGTTTCCCGTTAATACGG
KHP57	GAAGAAAGATAAAGAATTGG
KHP58	TATTTATCCCCGTACTTACG
KHP62	TATACCTACAGTGCTTTACC
KHP63	TCAACGAAAAACAAAGAAGC
KHP64	ACAAGGAAATTCAAAGTAGCC
KHP65	CTACCATTTTTTCAGCCAAT
NilD 5' ApaI	AAAGGGCCCTCTACCATTTTTTCAGC
NilD 3' KpnI	AAAGGTACCCTAGATATGCAAACTTC
SR-2 Websteri 5'	ATTTCCCCGCCGGATTAATATGCCAAAACCT
SR-2 Websteri 3'	CGTACTTACGGGGAACACATCATTGCCTGAACA
RPA Probe SDM 5'	CCATAGCTCCTTTAAATTTCCTTGATTATAACTCCATGTTCCCCG
RPA Probe SDM 3'	CGGGGAACATGGAGTTATAATCAAGGAAATTTAAAGGAGCTATGG
27F	AGAGTTTGATCATGGCTCAG
1492R	TACGGTTACCTTGTTACGACTT
Primer Extension and Northerns	
AAP1	CCGTACTTACGGGGAACATGG
AAP2	GGAGTTATAAACAAGGAAATTC
Mutant Construction	
dNilD Up 5' SalI	AAAGTCGACTGTCGCCCAATGCG
dNilD Up 3' ApaI	AAAGGGCCCTACTATTCGT
dNilD Dwn 5' ApaI	AAAGGGCCCGAATCCGTTCTATTC
dNilD Dwn 3' SacI	AAAGAGCTCAATTCCAACCTGACTCCG
Kan 5' ApaI	AAAGGGCCCCCACGTTGTGTCTCAAAATCT CTG
Kan 3' ApaI	AAAGGGCCCTTAGAAAAACTCATGGAGCATCAAATG
Cas3UpFwd_SpeI	ATATATACTAGTCCATGGCTACTTTGAATTTCCTTG
Cas3DownRev_XbaI	ATATATTCTAGACGGATTCCACCGATAGGGTG
Kan-Clean Rev_EcoRV_NEW	ATATATGATATCTTAGAAAAACTCATCGAGCATC AAATG
Kan-FullFwd NheI_NEW	ATATATGCTAGCCCACGTTGTGTCTCAAAATCTCTG
casEUpF_SpeI	ATATATACTAGTCTTTACCGCCGTGGACGAT
casEDownR_ XbaI	ATATATTCTAGAATAAAGGTTTACCCGTGTGCAGA
casEDownF_EcoRV	ATATATGATATCGATTCAGGCAAACAGCGGC
casEUpR2_NheI	ATATATGCTAGCGCAAGGTGACTTTAGACAG ATACA
NilD SDM set 1F (bases 2-3)	CGGGAATAAACCATGGCCACCTTGAATTTC CTTGTT
NilD SDM set 1R (bases 2-3)	AACAAGGAAATTCAAGGTGGCCATGGTTTAT TCCCG
NilD SDM set 2F (bases 4-5)	GAATAAACCATGGCCACCTTAAACTTCCTTG TTTATAAC
NilD SDM set 2R (bases 4-5)	GTTATAAACAAGGAAGTTTAAGGTGGCCAT GGTTTATTC
NilD SDM set 3F (bases 6-7)	CCATGGCCACCTTAAACTTTCTCGTTTATA ACTCCATG
NilD SDM set 3R (bases 6-7)	CATGGAGTTATAAACGAGAAAGTTTAAGGT GGCCATGG
NilD SDM set 4F (bases 8-9)	GCCACCTTAAACTTTCTCGTGTACAACTCC ATGTTCCCC
NilD SDM set 4R (bases 8-9)	GGGGAACATGGAGTTGTACACGAGAAAGTT TAAGGTGGC
NilD SDM set 5F (bases 10-11)	CTTAAACTTTCTCGTGTACAATTCTATGTTCCC CGTAAGTAC
NilD SDM set 5R (bases 10-11)	GTACTTACGGGGAACATAGAATTGTACACGAGA AAGTTTAAG
CasE 5' XbaI	AAATCTAGACCGATGTATCTGTCTAAAGTCACC
CasE 3' EcoRV	AAAGATATCCCATTACAGCGCCCTTATCAG
Vector Construction	
TOPO2.1mini_ Fwd_NcoI	ATATATCCATGGCGATGCCTGC
TOPO2.1mini_ Rev_NcoI	ATATATCCATGGTCCATTCGCCATTCAGGC
pECM20_Xb_F	GGGCCCGGATCAGATCTCGTTGTGTCTCA
pECM20_Xb_F	GGGCCCNNNNGGTACCGTGTCGACCTGCAGATGGAGA
pECMXb_insert_F	GGGCCCAGACGACATTGGCTGACTTGA
pECMXb_insert_R	GGTACCAAACCTAAATCACAAAAAGCACA
pECMXb_seq_F	AGGCCGGATAAAACTTGTGC
pECMXb_seq_R	TGGGACAACTCCAGTGAAGAG
pECMXb_integration_F	ATTGTTGATCGTGAGAAGTCG
pECMXb_integration_R	CTCCAATAAAGCGAATCCAG

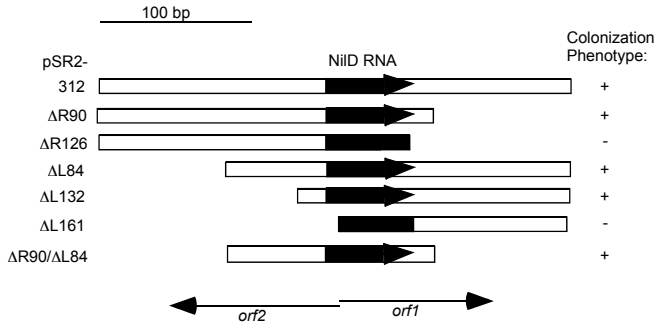

Supplemental Figure 1. Deletion analysis of the *nilD* region indicates neither *orf1* nor *orf2* is required in its entirety to rescue the colonization defect of the *nilD6*::Tn*5* mutant in plasmid complementation assays. Schematic representations of the deletion constructs tested for their ability to complement the colonization defect of the XnSc HGB081 nilD6::Tn5 mutant. The name of the plasmid carrying each fragment is shown on the left and is named according to whether the deletion truncates the 5' (ΔL) and/or 3' (ΔR) ends, and the size of the deleted region. *orf1* and *orf2* positions are indicated by arrows at the bottom of the figure, and the region encoding the 58-nt NilD RNA (see main text and Fig. 1) is shaded in black, with an arrow representing the full NilD RNA sequence and a rectangle indicating a truncation of the NilD RNA coding sequence. The colonization phenotype of XnSc HGB081 *nilD6*::Tn*5* carrying each plasmid construct is indicated to the right (see Table S3 for data).

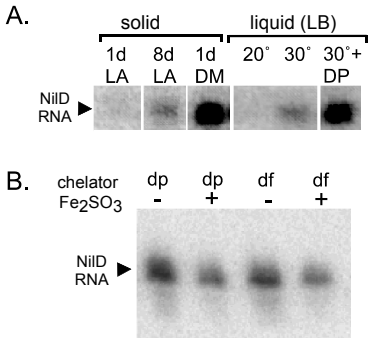

Supplemental Figure 2
A) NilD RNA expression under various conditions. Protection assays were performed with RNA isolated from wild-type HGB081 cells cultured on solid (lanes 1-3) or liquid (lanes 4-6) medium. RNA was isolated from cells growing on LA for 1 (lane 1) or 8 (lane 2) days or on solid defined medium (DM) for 1 day (lane 3). Cells were grown in liquid LB at 20˚C (lane 4) or 30˚C (lane 5) or in LB supplemented with 2,2-dipyridyl (DP) at 30˚C (lane 6). A representative experiment is shown; similar results were obtained in 2 independent experiments. Little NilD RNA-protected fragment was observed on LA plates after 1 d of incubation, with substantially more at 8 d, suggesting NilD RNA is elevated in nutrient-limited or aged cells. Indeed, NilD RNA was more abundant in X. nematophila incubated 1 d on a solid defined medium (see experimental procedures) than in 1 d LA plates (compare lanes 1 and 3), further suggesting that NilD RNA abundance is affected by nutrient availability. The elevated levels of NilD RNA do not appear to be the result of slow growth, since higher levels were not observed in cells grown at 20˚C relative to cells grown at the optimal X. nematophila growth temperature (30˚C). Instead, increased NilD RNA levels may be triggered by iron limitation since higher levels were detected after growth in LB supplemented with 2, 2-dipyridil (an Fe(II) chelator) than in LB alone (compare lanes 5 and 6).

B) NilD RNA expression during growth with iron chelators. Protection assays were performed with RNA isolated from wild-type HGB081 cells cultured in LB + 2,2-dipyridyl (lane 1, dp, -), LB + 2,2-dipyridyl + Fe2SO3 (lane 2, dp, +), LB + deferoxamine (Lane 3, df, -), or LB + deferoxamine + Fe2SO3 (lane 4, df, +). A representative experiment is shown; similar results were obtained in 2 independent experiments. RNA (i.e. protected fragment) levels similar to that found in LB grown cultures (data not shown) were observed in X. nematophila cells grown in the presence of iron chelators specific for Fe(II) or Fe(III) without exogenously added iron (Average ± SD, n=2, radioactivity relative to growth in LB: Deferoxamine, 1.19 ± 0.14; 2,2-dipyridyl, 0.94 ± 2.0). This result is in contrast to those obtained and shown in Fig. S2A, in which RNA levels were higher in the presence of chelator than in its absence. However, levels of iron in LB media preparations were not controlled, and it is likely that the LB-grown cells shown in Fig. S2B had already begun to experience iron limitation when they were harvested. Indeed, when Fe2SO3 was included in addition to the iron chelators the level of protected fragment was lower than that during growth in LB alone (Average ± SD, n=2, radioactivity relative to growth in LB: Deferoxamine + Fe2SO3, 0.54 ± 0.06; 2,2-dipyridyl + Fe2SO3, 0.59 ± 0.03). No protected fragments were detected in samples of RNA isolated from HGB315 nilD6::Tn5 cells grown under each of these conditions (data not shown).

Within each panel, all samples were run on a single gel, but for A, irrelevant lanes were removed by manipulation in Adobe Photoshop after visualization was enhanced through contrast.

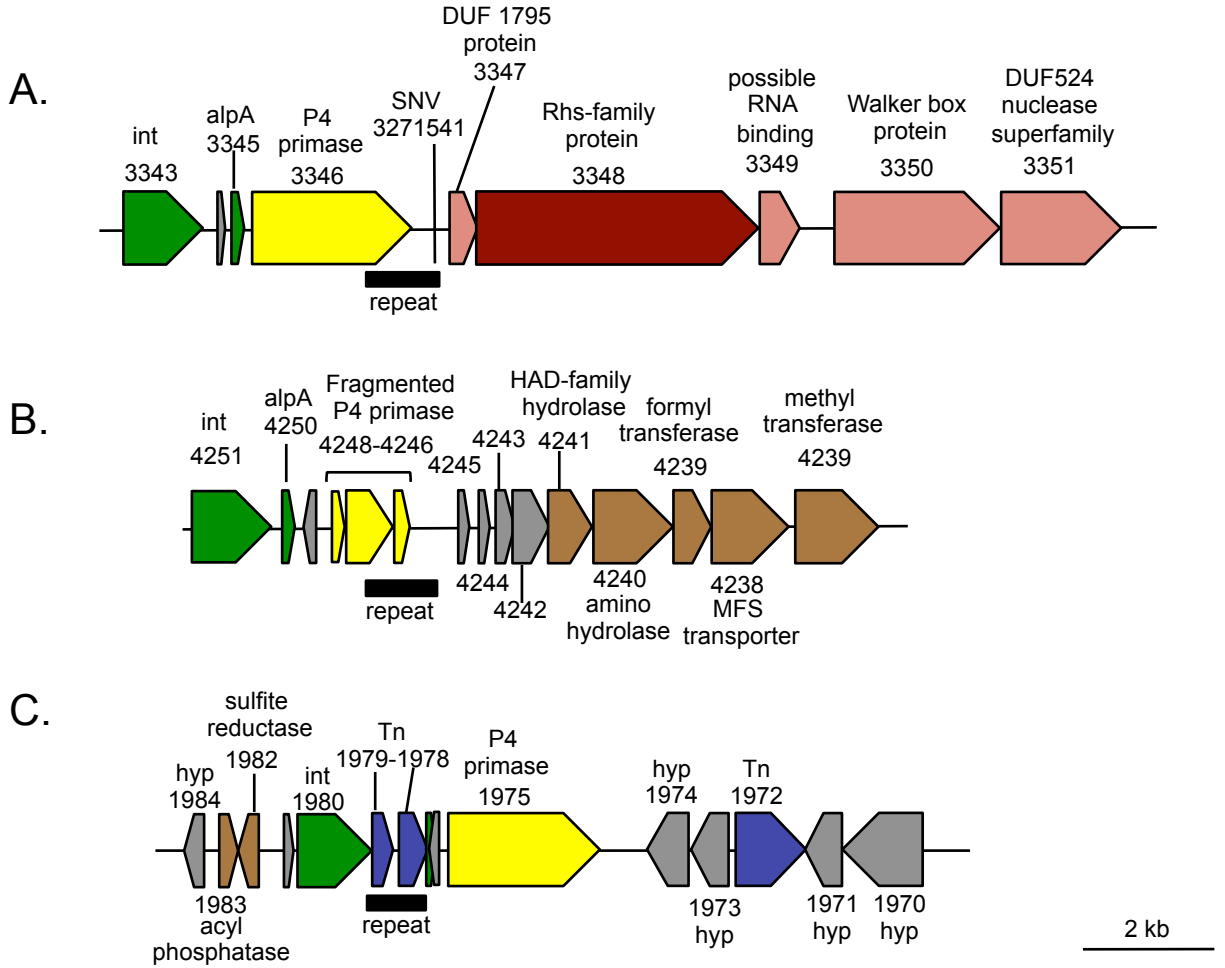

Supplemental Figure 3 (A) Genomic context of the single nucleotide variant (SNV), C-3271541-T, that distinguishes the *nilD6*::Tn*5* strain background from the XnSc 081 parent background. The SNV occurs within a 1147-bp sequence (black rectangle) that is repeated in two other regions of the genome, one at full length (**B)** and the other truncated by 208-nt (**C)**. Predicted open reading frames (box arrows) are labeled with their XNC1_ORF designation and predicted putative function. The boxes representing predicted P4 primases encoded at each locus are yellow whereas additional predicted functional categories are indicated by the following color scheme: Maroon (Rhs-family protein); Light red (potential Rhs-related proteins); Green (phage-related); Brown (metabolic); Blue (transposon and IS elements); Gray (hypothetical ORFs). A 2-kb scale bar for A-C is shown on the lower right. **(D)** Alignment of 40-nt of the repeat region surrounding the SNV (red underlined nucleotide). Within the 40-nt, sequence differences among the three repeats are highlighted as blue text and asterisks mark indels.